


M. MALDOVAN
M.R. BOCKSTALLER
E.L. THOMAS 
W.C. CARTER

Validation of the effective-medium approximation for the dielectric permittivity of oriented nanoparticle-filled materials: effective permittivity for dielectric nanoparticles in multilayer photonic composites

Department of Materials Science and Engineering, Massachusetts Institute of Technology, Cambridge, 02139 MA, USA

Received: 11 November 2002/Revised version: 28 April 2003
Published online: 9 July 2003 • © Springer-Verlag 2003

ABSTRACT A formula for the effective permittivity for two-dimensional particles embedded in a host matrix is derived and a method for its numerical evaluation is described. The method is applied to specific cases of circular, square, rectangular and triangular particles. Shapes are assumed for the inclusion particles. Data for obtaining the effective permittivity is provided for a wide range of filling fractions, geometries and dielectric contrasts between the particles and the matrix under the assumption of the quasi-static approximation, that is, the wavelength of the electric field is assumed to be much larger than the particle size. Metallic particles with complex and frequency-dependent dielectric constants are treated, as well as no-loss dielectric inclusions. Calculations are validated by comparing the results of the reflectivity obtained for a composite layer using the transfer-matrix method, assuming the layer to be an effective medium, to those using the finite-element method and accounting for the heterogeneous material.

PACS 78.20.-e; 78.20.Bh; 78.20.Ci; 78.66.Sq; 78.66.Vs

1 Introduction

The artificial engineering of microstructured materials has been the focus of extensive research because of the opportunities that arise for controlling the propagation of electromagnetic waves, especially through the creation of band-structure-like dispersion relations [1–3]. Whereas most studies have focused on photonic crystal properties, that is on the material properties in the frequency region in which the dispersion relation exhibits a band gap, the technological importance of microstructured materials arises in equal importance in the frequency regimes below the gap, where the dispersion relation is close to linear. Here, possible applications of periodically microstructured materials as classical optical elements, such as polarizers, prisms and lenses have been proposed [4, 5]. In this long-wavelength limit, the optical properties of artificial photonic materials may be custom tailored by choice of suitable material

composition and geometries, given that the optical properties of the periodic composite structures can be predicted with sufficient accuracy. Due to the linearity in the dispersion law, the Maxwell equations for the composite can be solved by replacing the periodic composite medium with an effective homogeneous medium [6]. Effective-medium theories have been constructed for various inhomogeneous media, in particular the fundamental Maxwell–Garnett approximation has been improved and generalized for various configurations [7, 8]. However, in many practical situations, application of the effective-medium approximation is problematic, because except for a few simple particle shapes such as spheres and ellipsoids, closed-form results have not been obtained. Also, the composite morphologies do not necessarily exhibit a homogeneous distribution of the dispersed component. Therefore, effective-medium results are indeterminate for arbitrary composite architectures [9]. As a consequence, the uncertainty about the applicability of effective-medium concepts is very unsatisfactory and approximations to geometries that are encountered in microstructured materials need careful examination. Given the increased number of applications of composites containing relevant spherical-shaped inclusions, for example two-dimensional wave-guiding structures, careful consideration of the modeling assumptions that are employed to design nanocomposite optical materials is necessary. Different approaches have been devised to study the effective response functions of two-dimensional composite materials, mainly based on the plane-wave expansion method [10–12]. While these approaches allow the determination of the effective response functions of composite materials with even intermediate filling fractions, they involve extensive numerical efforts and imply semi-infinite morphologies.

In this contribution, we present a method for calculating effective dielectric constants in composites with arbitrary two-dimensional particulate shapes and finite periodicity. The method is applied for several geometries that are similar to those being used in current applications and results are given for representative metallic and dielectric nanoparticle material compositions. We provide the numerical parameters that are necessary in order to practically evaluate the effective

response functions of the composite morphologies under consideration. Finally, the inherent accuracy of replacing a microstructured heterogeneous dielectric composite with an homogeneous effective medium is assessed by comparison of a finite-element calculation that resolves individual heterogeneities in a particulate composite to one that represents the particulate composite as a uniform phase with homogeneous effective dielectric constant. This allows us to critically assess the predictive accuracy of effective-medium calculations for refractive index engineering. Inclusion of nanoparticles in matrices has numerous applications in the area of optics. One such area is that of refractive index engineering. The ability to control the refractive index of materials has strong implications from chip optical circuits to photonic crystals. The introduction of nanoparticles into various matrices will allow the control of the refractive index and is dependent on a variety of parameters such as the filling fraction, geometry and index contrast of the system. The calculation for such optical nanocomposites is seemingly not straightforward. However, the use of an effective-medium approximation vastly simplifies this procedure and is shown to yield accurate results. In this context the medium is treated as macroscopically homogeneous and is assigned an effective permittivity that characterizes the system completely. This effective permittivity depends on the known dielectric constants and volume fractions for the matrix and the inclusions. However, closed analytical solutions for the problem can be obtained only for a few geometrical systems where the inclusions are spheres or ellipsoids [1]. In this paper, a finite-element numerical approach is used to obtain effective permittivities for several two-dimensional shapes that can be used on photonic crystal composites.

2 Effective-permittivity model

In this section, the effective-permittivity model for a composite material is presented. The effective permittivity is determined by the particle and matrix dielectric functions as well as particulate shapes and volume fractions.

Consider a composite for which the background host material has a dielectric constant ϵ_m . The displacement field \mathbf{D} is then given by:

$$\mathbf{D} = \epsilon_m \mathbf{E} + \mathbf{P}, \quad (1)$$

where \mathbf{E} is the electric field and \mathbf{P} is the polarization of the particles.

The effective permittivity of the composite is then defined as

$$\mathbf{D} = \epsilon_{\text{eff}} \mathbf{E}. \quad (2)$$

Using (1) and (2) yields

$$\epsilon_{\text{eff}} \mathbf{E} = \epsilon_m \mathbf{E} + \mathbf{P}. \quad (3)$$

The polarization \mathbf{P} is assumed to be a linear isotropic function of the local electric field:

$$\mathbf{P} = N\alpha \mathbf{E}_L, \quad (4)$$

where N is the number of particles per unit volume, α is the polarizability of an individual particle and \mathbf{E}_L is the local electric field ‘seen’ by an inclusion. It is the sum of two contributions; the electric field from exterior sources \mathbf{E} and the electric field created by the other particles.

The local field is given by Yaghjian [13] for arbitrarily shaped particles:

$$\mathbf{E}_L = \mathbf{E} + \frac{\overline{\overline{\mathbf{L}}} \cdot \mathbf{P}}{\epsilon_m}, \quad (5)$$

where $\overline{\overline{\mathbf{L}}}$ is the source dyadic that depends on the particle shape of the inclusions.

If it is assumed that the particles have the same shape and their principal axes are oriented in the same direction, uniformly aligned along preferred orientations, then as a result the polarizability α becomes a diagonal tensor represented by α_i . By combining (3), (4) and (5), the expression for the effective permittivity is obtained:

$$\epsilon_{\text{eff},i} = \epsilon_m + \epsilon_m \frac{N\alpha_i}{\epsilon_m - L_{ii}N\alpha_i}, \quad (6)$$

where $i = x, y, z$ are the Cartesian directions.

The principal components of the polarizability α_i of the particles needs to be calculated numerically for arbitrary particle shapes. The particle dimension is assumed to be much less than the wavelength of the electromagnetic radiation (quasi-static approximation). The internal field approach, in which polarizability is obtained by solving the internal field \mathbf{E} of the particle, is used so that the dipole moment \mathbf{p} of a particle with dielectric constant ϵ_p , in an infinite homogeneous region with dielectric constant ϵ_m , is calculated as:

$$\mathbf{p} = \int_V (\epsilon_p - \epsilon_m) \mathbf{E} dV, \quad (7)$$

where the integration is carried out only within the volume of the particle.

The dipole moment \mathbf{p} is defined as the product of the polarizability α and the local field \mathbf{E}_L . For this system, unbounded in an infinite medium, the local field \mathbf{E}_L and the external field \mathbf{E} can be shown to be the same [14]. Considering ϵ_p to be constant throughout the particle volume of the inclusion, the dipole moment can be written as:

$$\mathbf{p} = (\epsilon_p - \epsilon_m) V \frac{\int_V \mathbf{E}_{\text{INT}} dV}{V}, \quad (8)$$

where the internal electric field is integrated within the particle. In this region, the internal electric field vector has x, y, z -components but its integral over the volume of the particle will have only one component for symmetric particles that are properly aligned with respect to the external electric field. Moreover, if we align the applied electric field along a Cartesian direction i , and define β as the integral of the internal electric field over the particle volume divided by its volume and the external electric field, we can write

$$\mathbf{p}_i = (\epsilon_p - \epsilon_m) V \beta_i \mathbf{E}_{\text{EXT},i}. \quad (9)$$

The integral β is hence independent of both the particle volume and the external electric field. It can be determined numerically and relates to the effect of particle shape on the local field. Replacing α_i in (6) by $(\varepsilon_p - \varepsilon_m)V\beta_i$, the final equation for the expression that is convenient for numerical representation of effective permittivity is obtained:

$$\varepsilon_{\text{eff},i} = \varepsilon_m + \varepsilon_m \frac{f(\varepsilon_p - \varepsilon_m)\beta_i}{\varepsilon_m - L_{ii}f(\varepsilon_p - \varepsilon_m)\beta_i}, \quad (10)$$

with f denoting the filling fraction of the particles in the composite. β_i is reported in this paper for both metallic and dielectric particles of different two-dimensional shapes and for various dielectric contrasts between the matrix and the particles. A finite-element calculation that solves Maxwell's equations was performed to obtain the values of β [15]. Through the boundary conditions that define the electric potential along the finite-element mesh, the particle is placed in a homogeneous external electric field $\mathbf{E}_{\text{EXT},i}$ and all the components for the internal electric field are calculated. The integration of this internal field is carried out only over the volume of the particle, giving the value of β after dividing by the particle volume and the respective external electric field.

We note that in the case of circular cylindrical geometry, the resulting value of β can be compared to the analytical one, that is $\beta = 2/(\varepsilon_p/\varepsilon_m + 1)$ [17].

3 Effective-permittivity calculations for 2D periodic heterogeneous materials

In this paper, the study of effective permittivities for dielectric heterogeneous composites is focused on photonic applications. It is known that experimental observations indicate that the inclusion of particles within a matrix in a layer of lower dielectric constant enhances its effective dielectric constant. This effect has been used for example to engineer the dielectric constants of individual layers in a multilayer photonic stack [18]. In the following, the effective permittivity of a two-dimensional composite layer is obtained for different particle shapes, dielectric contrasts and filling fractions. The accuracy of the effective-permittivity method is studied by comparing the results for normal-incidence reflectivity on that "effective" layer, against the reflectivity from actual numerical simulations of heterogeneous composites.

The two-dimensional shapes chosen for the numerical calculations consisted of circles, squares and rectangles of variable aspect ratio, and equilateral triangles. An example of such a heterogeneous layer is shown in Fig. 1. Note that the characteristic length scale of the particles is determined for each geometry via the filling fraction $f = Na$, where N is the number of particles per unit area and a is the area of a particle.

Since only normal incidence is considered, the incoming electromagnetic wave is assumed to travel along the x direction. The incoming electric field \mathbf{E} is along the z direction for TE polarization and along the y direction for TM polarization [19]. These orientations only define the boundary conditions for our calculations, however, due to the fact that



FIGURE 1 Schematic diagram of a heterogeneous layer in a two-dimensional photonic crystal. The system is infinitely periodic in the y direction

Maxwell's interface conditions must be satisfied at the interfaces, and the fields are considered to have any direction in the domain of our calculation. The effective permittivity for TE polarization is given by

$$\varepsilon_{\text{eff},z} = (1 - f)\varepsilon_m + f\varepsilon_p, \quad (11)$$

whereas, for TM polarization,

$$\varepsilon_{\text{eff},y} = \varepsilon_m + \varepsilon_m \frac{f(\varepsilon_p - \varepsilon_m)\beta_y}{\varepsilon_m - L_{yy}f(\varepsilon_p - \varepsilon_m)\beta_y}. \quad (12)$$

There will be no effective dielectric constant along the x direction due to the symmetric alignment of each particle with respect to the incoming electric field. The value of the source dyadic L_{yy} is equal to 0.5 for circular, square and equilateral triangular shapes, but for rectangular shapes, $L_{yy} = \frac{2}{\pi} \tan^{-1}(\frac{1}{R})$, where the aspect ratio R is defined as the ratio between the height and base ($R = h/b$) [16]. Here, it is assumed that h is oriented along the y direction and b is along the x direction. Now, the only parameter remaining unknown is β_y and therefore the effective properties are completely determined by the integral defined by β_y . β_y is calculated below for systems comprising a no-loss dielectric matrix and dielectric as well as for metallic particles of various geometrical shapes and frequency dependent refractive indices.

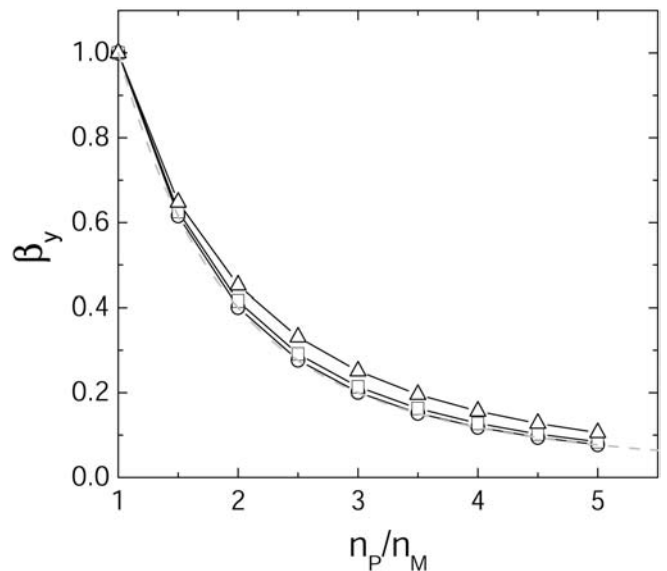


FIGURE 2 Plot of β_y for circular (\circ), square (\square) and triangular (\triangle) particles as a function of the dielectric contrast between particles and matrix. n_p corresponds to the refractive index of the dielectric particles and n_m to the matrix. The dotted gray line represents the Maxwell-Garnett approximation using the analytical expression for β assuming circular geometry (see text)

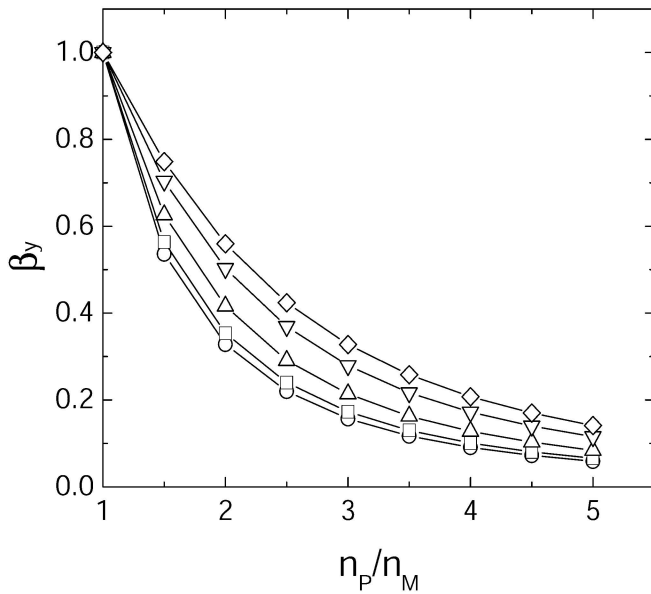


FIGURE 3 Plot of β_y for rectangular particles as a function of the refractive index contrast between particles and matrix and the aspect ratio R between height and base ($R = h/b$) with $R = 1/3$ (\circ), $1/2$ (\square), 1 (\triangle), 2 (∇), and 3 (\diamond). n_p corresponds to the refractive index of the dielectric particles and n_m to the matrix

3.1 No-loss dielectric

Each shape is characterized for values of the dielectric contrast, ranging between $n_p/n_m = 1$ and $n_p/n_m = 5$, where n is the refractive index ($\varepsilon = n^2$), n_m denotes the refractive index of the matrix and n_p the refractive index of the particles. This range of contrast covers the typical material compositions that are found in technological applications, for example SiO_2/Si , Si/air or chalcogenide glasses [21].

3.1.1 Circles, squares and triangles. The results for β_y in the case of circular, square and triangular shapes for varying dielectric contrast is shown in Fig. 2. β_y is independent of the length scale and depends only on the shape of the particles and the dielectric contrast between the particles and matrix. The sides of the squares are assumed to be oriented along the x and y directions and the equilateral triangles have one of their sides parallel to the y direction, as shown in the schematic in Fig. 5. Since the results for squares with the diagonal lines oriented along the x and y directions do not significantly differ from those rotated $\pi/4$ about their centers, only one limiting case is shown here. Note that the Maxwell–Garnett theory, assuming the analytical expression for β closely matches the numerical results obtained for the circular case. However, significant deviations from the numerical results occur for anisotropic particle shapes.

3.1.2 Rectangles. The values for β_y are independent of the size of the rectangle as long as its aspect ratio, R , is constant. The sides of the rectangles are considered to be oriented parallel to the x and y directions, as shown schematically in Fig. 5. Figure 3 summarizes the results obtained for β_y in the case of rectangular particle geometry, which have been obtained for different aspect ratios and different dielectric contrast between host material and inclusion.

3.2 Dielectric with loss

In the case of particles with dielectric loss, the dielectric constant $\varepsilon = \varepsilon_1 + i\varepsilon_2$ is a complex number with the

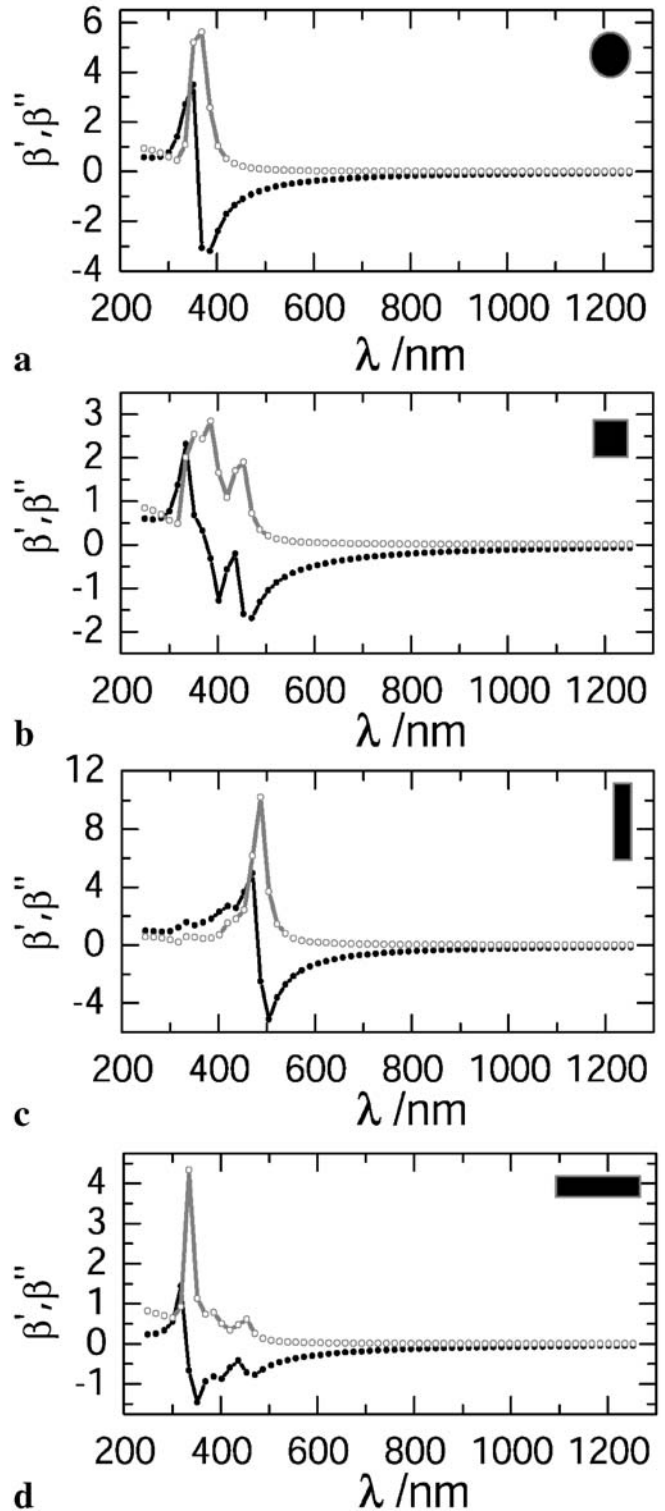


FIGURE 4 Plot of the complex β_y for silver metallic particles as a function of the wavelength. β' is the real part (black, \bullet), β'' is the imaginary part (gray, \circ). For rectangular shapes, the aspect ratio R between height and base is defined as $R = h/b$ and is set to be $R = 3$ (c) and $R = 1/3$ (d), respectively

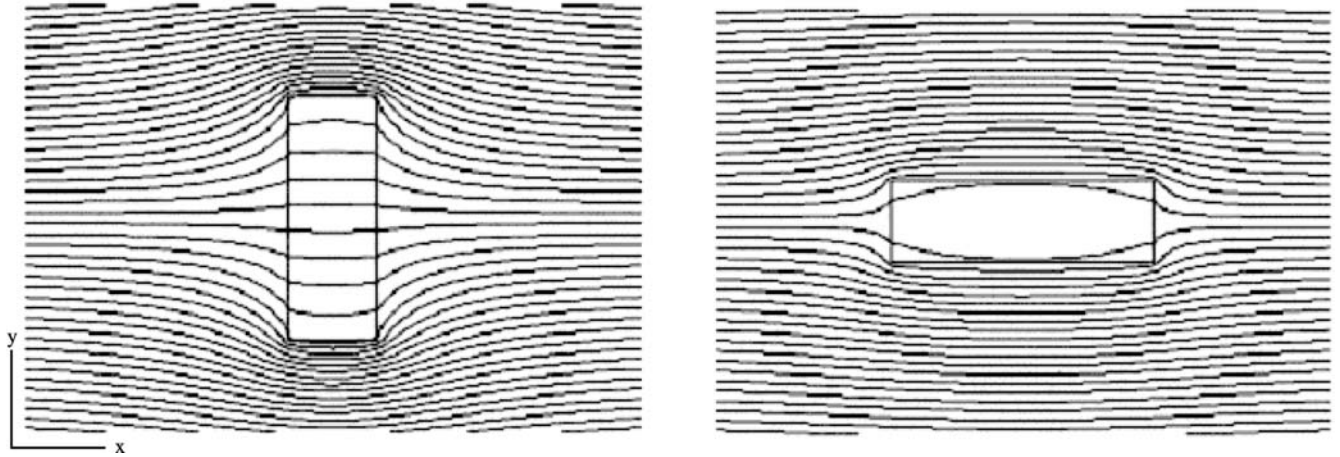


FIGURE 5 Schematic diagram of the equipotential lines representing the electric field distribution for a rectangular particle within an external electric field along the y axis. The electric field vector is normal to the equipotential lines and its magnitude is proportional to the density of lines. In both cases the dielectric contrast between the matrix and the particle is $\epsilon_p/\epsilon_m = 9$ and the aspect ratios are $R = 3$ and $R = 1/3$, respectively. The alignment with respect to the external electric field in the $R = 3$ case produces a higher electric field within the particle. As a result, a higher effective dielectric permittivity arises from this configuration

real ϵ_1 and imaginary parts ϵ_2 depending on the frequency of the electromagnetic radiation. An example calculation is provided below for the particular case of the inclusions being considered to be silver particles with the dielectric bulk properties of silver [21] and where the host medium is assumed to have a refractive index $n_m = 1.5$, corresponding to most polymeric materials or silica.

The results for the real and imaginary parts of β_y for the case of spherical, square and rectangular geometries are shown in Fig. 4 as a function of the wavelength. A pronounced frequency dependence of the real and imaginary parts of β_y is found for all geometries near the plasma frequency of silver ($\lambda_p = 350$ nm). For higher frequencies β_y vanishes, due to the large absorbance of the material. Evident from the data presented in Figs. 3 and 4 is a pronounced difference in the effect of horizontally and vertically aligned rectangular elements on the x parameter β . The anisotropic behavior of a rectangular particle can be rationalized as follows. As an example, consider for both cases of particle alignment the dielectric contrast between the matrix and the particle set equal to nine, with the electric field applied along the y axis. At the material interfaces, the boundary conditions must be respected, that is continuity of the tangential component of the electric field and continuity of the normal component of the displacement vector. Two configurations can be distinguished: in the first case, the larger dimension is aligned along the y direction. In this situation, by increasing h , the electric field within the particle will resemble the external electric field because of the requirement of tangential continuity. In the second configuration, the larger dimension is along the x axis. As β increases, the electric field within the particle would be along the y axis, but the magnitude will be one-ninth of the external electric field because of the requirement for continuity of the normal part of the displacement vector. Both situations are illustrated in Fig. 5. From these two limiting cases, it can be inferred that a vertical alignment in which the larger dimension mostly encounters a tangential electric field component will produce a higher internal electric field than a horizontal alignment in which the larger dimension mostly

faces a normal field component. As a result, alignment of the shorter dimension of the particle along the electric field direction will generally produce a higher effective dielectric permittivity.

4 Validation

To determine the validity and accuracy of (9), as well as the β_y values, we calculated the normal incidence reflectivity for different particle shapes for both an actual heterogeneous dielectric layer and the corresponding ‘effective’ layer. In the case of the heterogeneous layer, a finite-

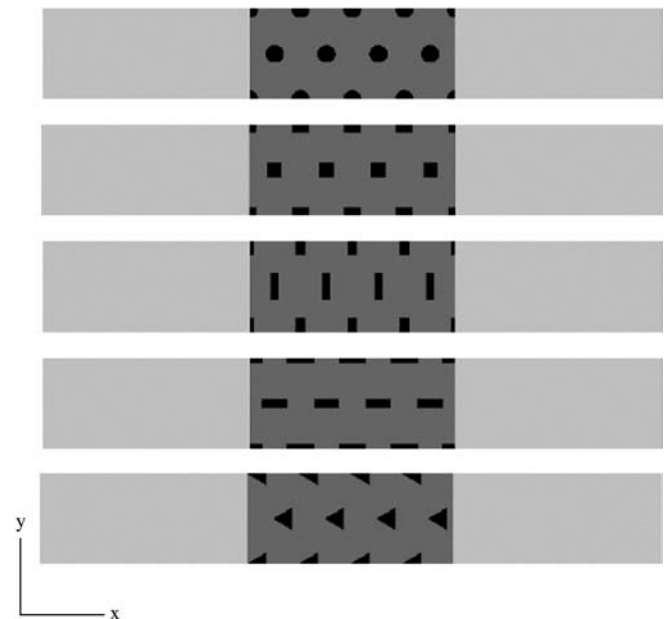


FIGURE 6 Schematic diagram of the heterogeneous composite layers used to calculate reflectivity by using the finite-element method. The layer thickness is 120 nm, the lattice constant is 30 nm, the filling fraction $f = 10\%$, $n_m = 1.5$, and $n_p = 7.5$. For rectangular particles the aspect ratios are $R = 3$ and $R = 1/3$, respectively. Light is incident along the x direction

element (FEM) code was developed to obtain the normal incidence reflectivity for two-dimensional structures [19, 20]. For the corresponding effective layer, reflectivity was calculated by using the one-dimensional transfer-matrix method (TMM) [16].

A representative filling fraction of 10%, a lattice constant of 30 nm and a single layer of thickness 120 nm were chosen for all cases. The unfavorable situation in which the refractive index contrast n_p/n_m between the particles and the matrix is equal to five is considered as a test case, since an extreme index contrast should exhibit the largest comparative errors. It is expected that the results would also be accurate when the contrast is lower.

The absolute reflectivity of the composite will depend on the dielectric constants of both components, matrix and particles.

The heterogeneous dielectric configurations considered for finite-element calculations are illustrated in Fig. 6. Note that perturbations of the positions of the particles from the

regular lattice are not expected to have a strong influence on the optical response of the composite as long as electrodynamic interactions between individual particles can be neglected. The range for the wavelengths of the incident electromagnetic waves was selected such that in all cases the particle dimension d was much less than the wavelength λ ($d/\lambda < 0.02$). For this situation, scattering losses can be neglected (quasi-static approximation). The results for normal-incidence reflectivity, that is for light incident along the x direction, from a single heterogeneous layer comprising no-loss dielectric inclusions of various shapes embedded within a dielectric host medium are shown in Fig. 7, and are compared against those reflectivity results from the corresponding effective layer. The difference in the calculated reflectivities obtained by the transfer-matrix method assuming an effective dielectric function for the composite and the finite-element model are less than 1% and cannot be distinguished in the graphs. The predictive accuracy of the effective-medium model, as obtained for the case of no-loss dielectric inclu-

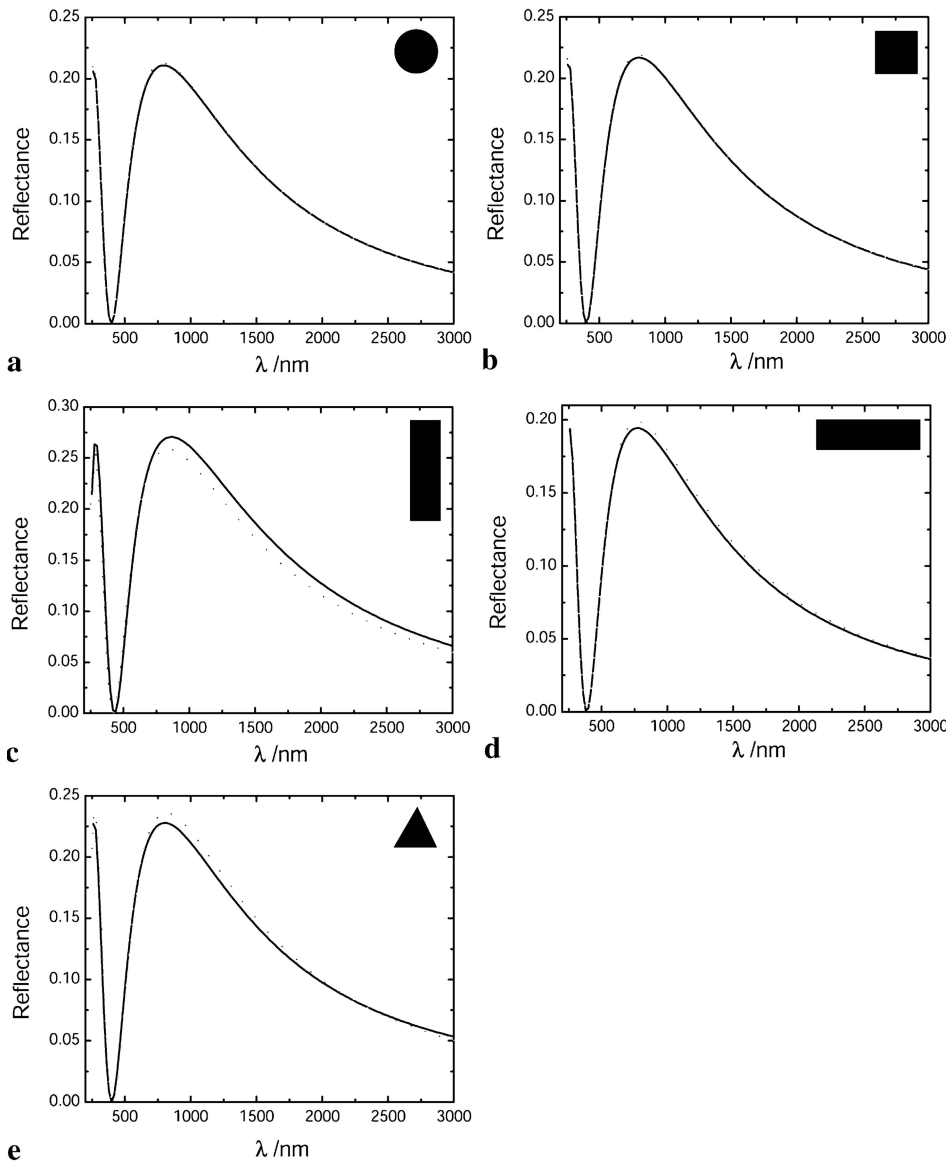


FIGURE 7 Comparison of the optical properties of a heterogeneous layer and an effective layer with no-loss dielectric inclusions. Reflectivity versus wavelength is calculated for an effective layer by use of the transfer-matrix method (black) and for a heterogeneous layer by use of the finite-element method (gray) for different particle geometries: circular (a), square (b), rectangular ($R = 3$) (c), rectangular ($R = 1/3$) (d) and triangular (e). For all cases, $n_m = 1.5$, $n_p = 7.5$, and the filling fraction is $f = 10\%$. The effective refractive indices are $n_{\text{EFF}}(\text{circles}) = 1.647$, $n_{\text{EFF}}(\text{squares}) = 1.661$, $n_{\text{EFF}}(\text{rectangles } R = 3) = 1.752$, $n_{\text{EFF}}(\text{rectangles } R = 1/3) = 1.615$ and $n_{\text{EFF}}(\text{triangles}) = 1.701$

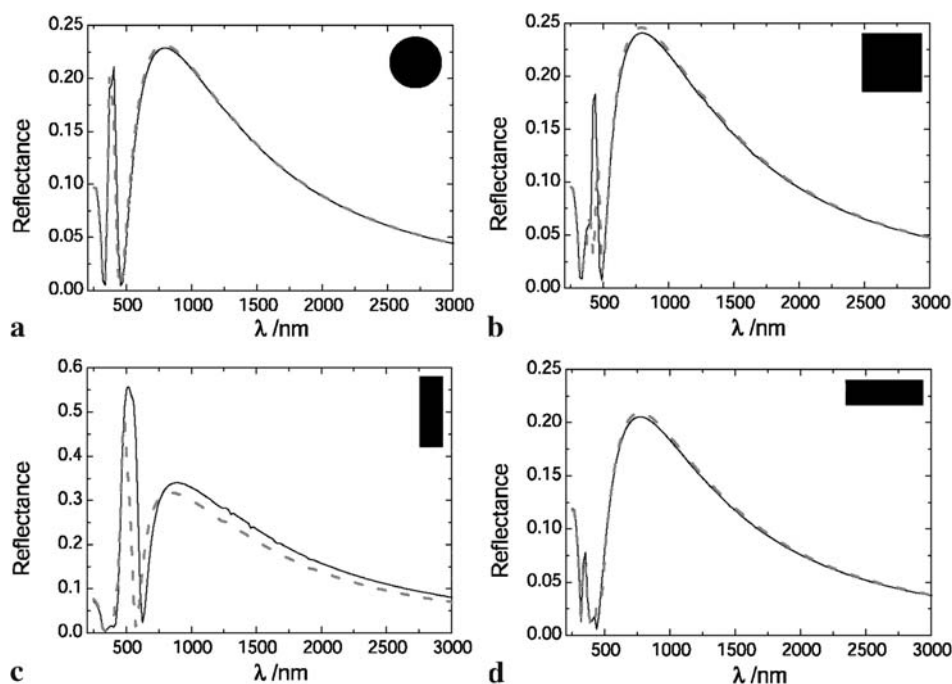


FIGURE 8 Comparison of the optical properties of the heterogeneous and effective layers with lossy metallic inclusions. Reflectivity versus wavelength is calculated for the effective layer by use of the transfer-matrix method (*black*) and for the heterogeneous layer by using the finite-element method (*gray*) for different particle geometries: circular (**a**), square (**b**), rectangular ($R = 3$) (**c**) and rectangular ($R = 1/3$) (**d**). For all cases, $n_m = 1.5$ and the filling fraction is $f = 10\%$. The optical properties of the particles are assumed to be equal to those of the bulk properties of silver, as tabulated in [21]

sions, however, is significantly reduced in the case of strongly absorbing metallic inclusions. Figure 8 shows the comparison of the calculated reflectivity of a heterogeneous layer comprising silver inclusions of varying geometry embedded within a no-loss dielectric host material. Here, the optical constants of silver have been assumed to be equal to those of bulk silver, as given by Palik [21]. Significant deviations are only apparent in the case of the rectangular geometry with an aspect ratio $R = 3$, for which the effective-medium theory underestimates both the absolute value of reflection as well as the wavelength of maximum reflectivity. This can be understood, following the arguments presented above, by the pronounced field distortion in the case of particle alignment along the electric field direction, resulting in electromagnetic interactions between individual inclusions not taken into account by the effective-medium theory.

5 Conclusions

Effective-medium theory provides a valuable tool for the rapid evaluation of the optical properties of microstructured nanocomposites of various particle shapes, while avoiding extensive numerical calculations. Within the material compositions and geometries studied above, numerical methods for extracting effective-medium optical constants allow the rapid evaluation of microstructured composite 2-D composite designs. In our paper we have shown that effective-medium concepts can be applied to composite materials where the dispersed component has a non-spherical shape, and that these effective-medium concepts are of high predictive accuracy in the case of no-loss dielectric inclusions. Increasing deviations from the analytical result assuming circular particle geometry are found if anisotropic particle shapes are considered. For strongly absorbing metallic components, effective-medium theory results in significant errors in the estimation of the material response function. This

is demonstrated by the comparison between the reflectivity values of a nanocomposite layer calculated using effective-medium theory and the finite-element method. It is shown that the effective-medium approach accounts for the properties of composite materials containing dielectric triangular-, square-, circular- or rectangular-shaped particles within 1%, and within about 10% for metallic particles at moderate particle filling fractions. The critical filling fraction for which the effective-medium theory breaks down was shown to depend on the geometry of the particle as well as on its absorbing characteristics.

The results presented in this paper justify the application of effective-medium concepts to the calculations of optical properties of nanocomposite materials containing non-spherical-shaped inclusions, which are likely to gain increasing importance in the field of photonic applications.

ACKNOWLEDGEMENTS M. Maldovan and W.C. Carter would like to acknowledge the financial support of the Singapore–MIT alliance. Furthermore, this material is based upon work supported by, or in part by, the U.S. Army Research Laboratory and the U.S. Army Research Office under Contract No. DAAD-19-02-0002, as well as by the Alexander von Humboldt Foundation (Feodor–Lynen program).

REFERENCES

- 1 J.D. Joannopoulos, R.D. Meade, J.N. Winn: *Photonic Crystals – Molding the Flow of Light* (Princeton University Press, Princeton, New Jersey 1995)
- 2 E. Yablonovitch: *Phys. Rev. Lett.* **58**, 2059 (1987)
- 3 S. John: *Phys. Rev. Lett.* **58**, 2486 (1987)
- 4 S.Y. Lin, V.M. Hietala, L. Wang, E.D. Jones: *Opt. Lett.* **21**, 1771 (1996)
- 5 H. Kosaka, T. Kawashima, A. Tomita, M. Notomi, T. Tamamura, T. Sako, S. Kawakami: *Phys. Rev. B* **58**, R10 096 (1998)
- 6 T.C. Choy: *Effective-Medium Theory – Principles and Applications* (Oxford University Press, Oxford 1999)
- 7 J.C. Maxwell-Garnett: *Philos. Trans. R. Soc. London Ser. A* **203**, 385 (1904)

- 8 K. Busch, C.M. Soukoulis: *Phys. Rev. Lett.* **75**, 3442 (1995)
- 9 A. Priou: *Dielectric Properties of Heterogeneous Materials* (Elsevier, New York 1991)
- 10 S. Datta, C.T. Chan, K.M. Ho, C.M. Soukoulis: *Phys. Rev. B* **48**, 14 936 (1993)
- 11 A.A. Krokhin, P. Halevi, J. Arriaga: *Phys. Rev. B* **65**, 115 208 (2002)
- 12 H.F. Contopanagos, C.A. Kyriazidou, W.M. Merrill: *J. Opt. Soc. Am. A* **16**, 1682 (1999)
- 13 A.D. Yaghjian: *Proc. IEEE* **68**, 248 (1980)
- 14 A. Shivola, I.V. Lindell: *J. Electromagnetic Waves Applic.* **3**, 37 (1989)
- 15 A. Shivola, I.V. Lindell: *J. Electromagnetic Waves Applic.* **4**, 1 (1990)
- 16 J.D. Jackson: *Classical Electrodynamics* (Wiley, New York 1999)
- 17 F.J. Garcia-Vidal, J.M. Pitarke, J.B. Pendry: *Phys. Rev. Lett.* **78**, 4289 (1997)
- 18 E.R. Brown: *Appl. Phys. Lett.* **67**, 2138 (1995)
- 19 J.L. Volakis: *Finite Element Method for Electromagnetics* (IEEE Press, New York 1998)
- 20 P. Yeh, A. Yariv, C.S. Hong: *J. Opt. Soc. Am.* **67**, 423 (1977)
- 21 E.D. Palik: *Handbook of Optical Constants of Solids* (Academic Press, San Diego 1998)